Electronic Supplementary Material (ESI) for Journal of Materials Chemistry B.

Development of zwitterionic copolymers with multi-shape memory effects and moisture-sensitive shape memory effects

Shaojun Chen[1*], Funian Mo[1], Florian J Stadler[1],Shiguo Chen[1], Zaochuan Ge[1], Haitao Zhuo[2*]，

[1]*Shenzhen Key Laboratory of Special Functional Materials, Nanshan District Key Lab for Biopolymers and Safety Evaluation, College of Materials Science and Engineering, Shenzhen University, Shenzhen, 518060, China.* [2]*College of Chemistry and Chemical Engineering, Shenzhen University, Shenzhen, 518060, China.*

*Corresponding author: College of Materials Science and Engineering，Shenzhen University, Shenzhen 518060, China. Tel and Fax: +86-755-26534562. E-mail: S.J.Chen, chensj@szu.edu.cn; H.T.Zhuo, haitaozhuo@163.com;

Supporting information

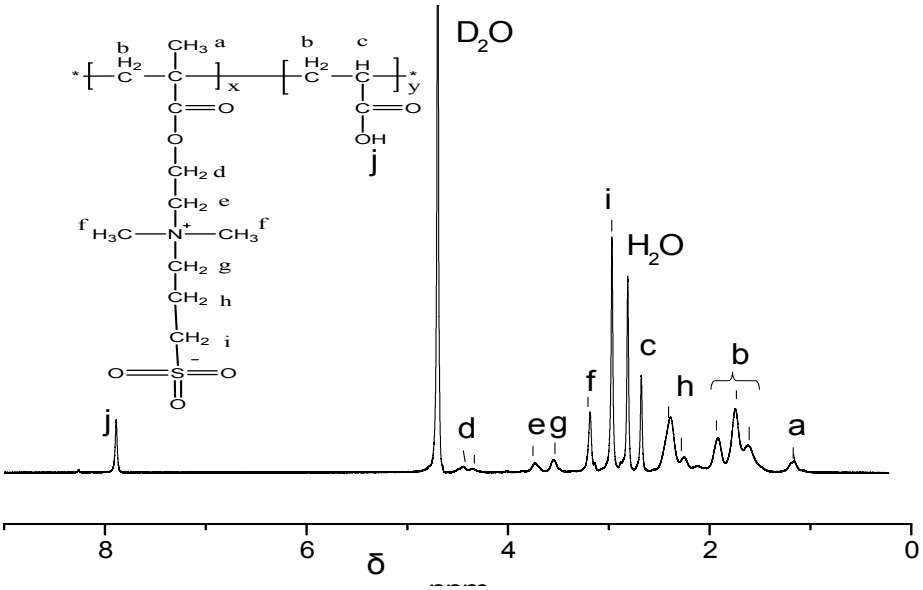

Figure SI1. NMR spectra of DMAPS-co-AA copolymer

The NMR spectrum further confirms that the peaks at δ = 1.1, 2.3, 2.9, 3.2, 3.5, 3.8, and 4.5 ppm can be ascribed to the protons at the *a*, *h*, *i*, *f*, *g*, *e,* and *d* sites of the DMAPS segments, respectively. The peak at δ= 2.66 ppm is ascribed to the proton at the *c* site of the AA segments. The peak at δ= 7.88 ppm is ascribed to the proton at the *j* site of the AA segments.[1] However, the peak at around 2.8ppm is ascribed to the proton of H_2O due to moisture absorption.

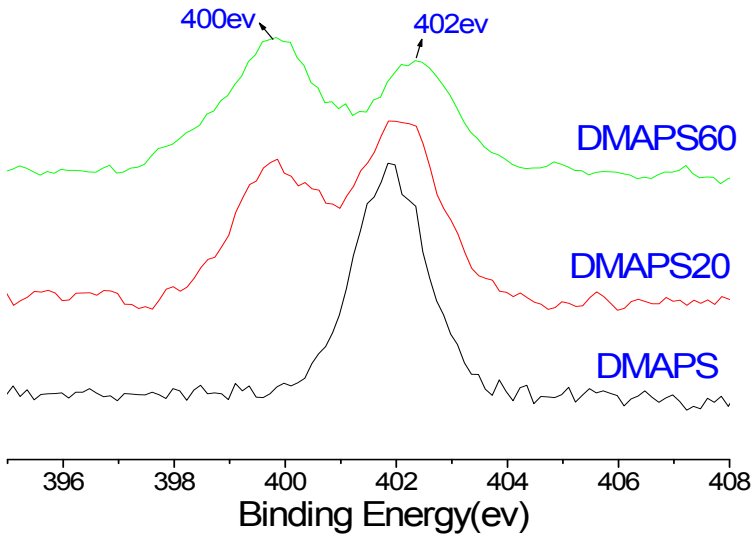

Figure SI2. XPS spectra of DMAPS-co-AA copolymer

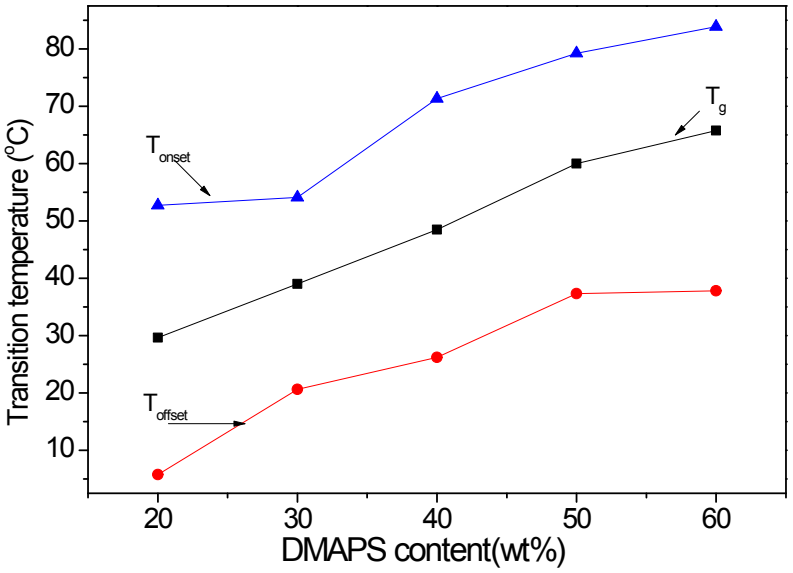

Figure SI3. The dependence of transition temperature (T_g, T_{onset}, T_{offset}) on DMAPS content

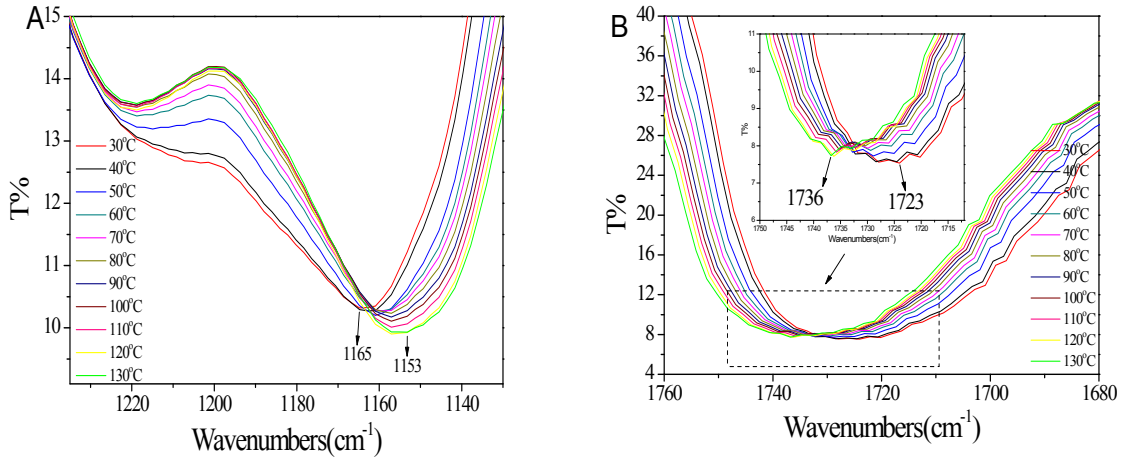

Figure SI4. Temperature dependent FT-IR spectra of sample DMAPS40 for (A) OH deformation vibration and (B) C=O stretching vibration

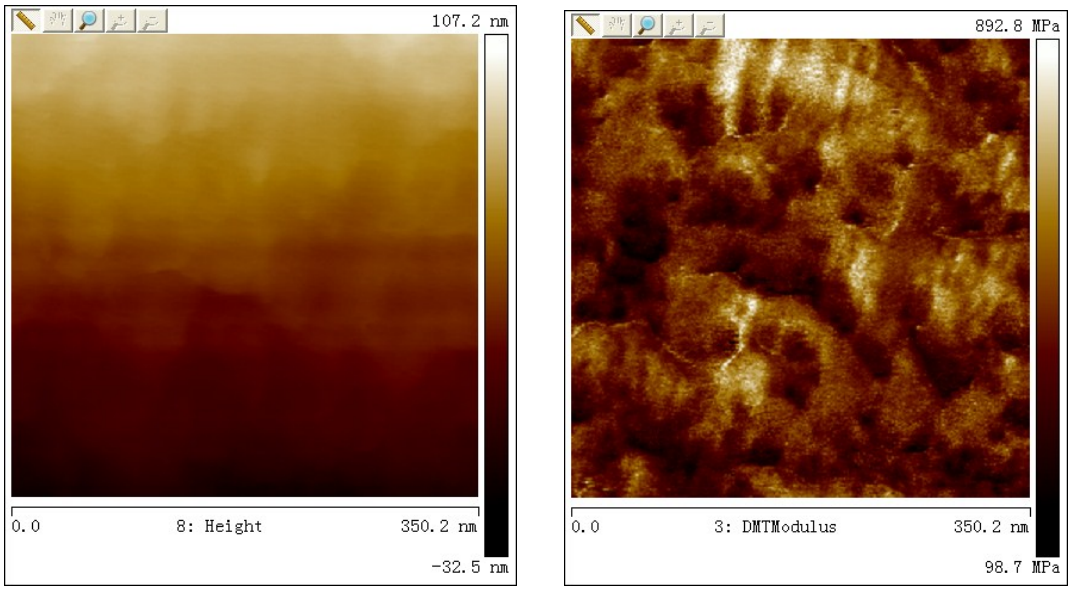

Figure SI5. AFM 2D-images (height and DMT-modulus) of p(DMAPS-co-AA)

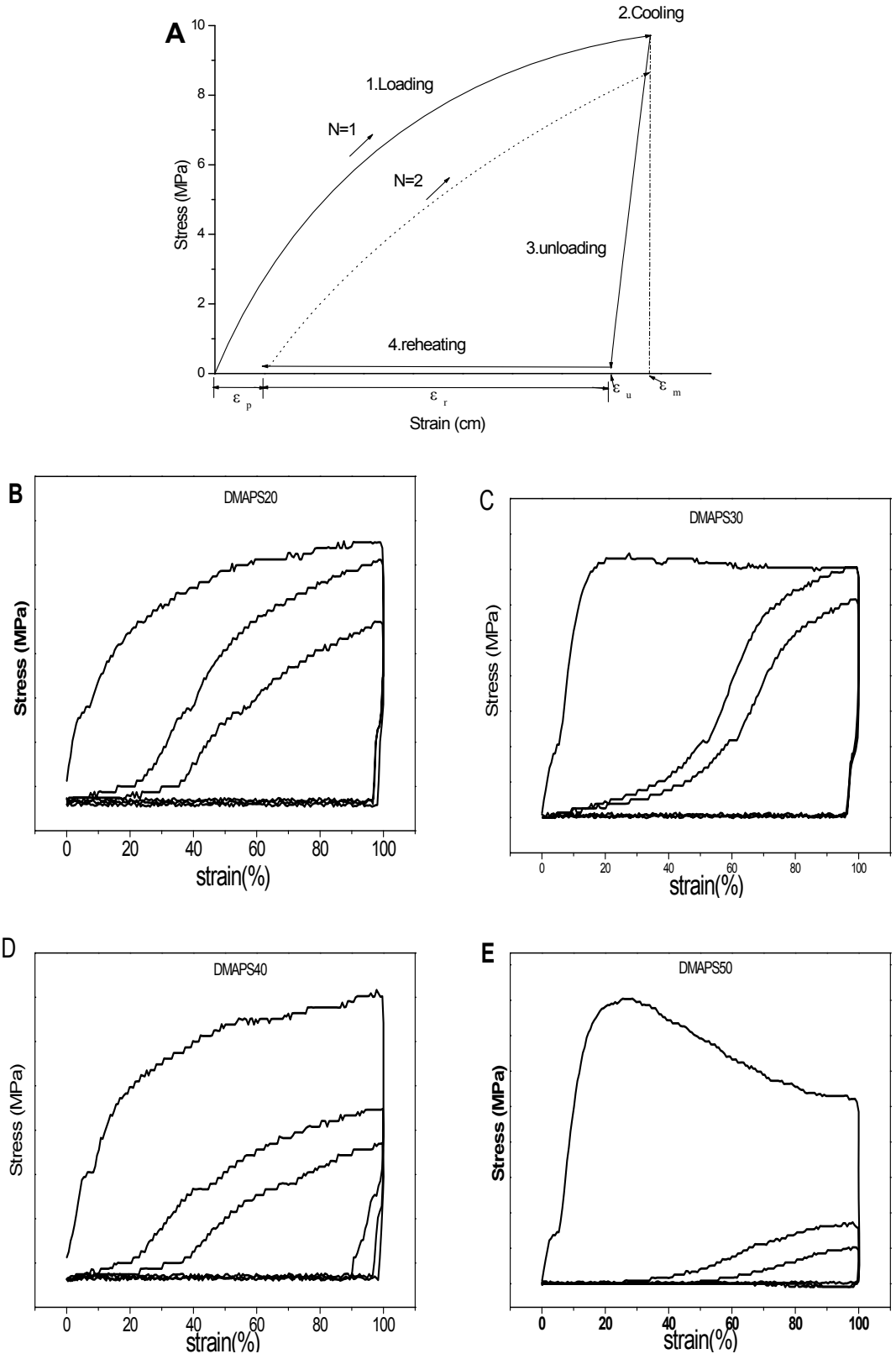

Figure SI6. Cyclic tensile testing method (A) and shape memory behaviors of p(DMAPS-co-AA) copolymers with different DMAPS content (B-E)

A cyclic tensile test was performed by using a mechanical tensile testing apparatus (SANS, China) with a controlled temperature chamber according to the procedure described in the literature.[2, 3] First, the specimen with 5mm width, 20mm length, and 0.5mm thickness was heated to T_{high}=80°C, within 600s. Then, the sample was stretched to ε_m, 100% elongation at T_{high}, with a 10mm/min stretching rate. Second, cool air was introduced into the chamber to cool the sample with a constant strain ε_u to T_{low}=20°C within 900s. Thereafter, the strain was released from ε_u to ε_p with subsequent heating to 80 °C for 600 s. This sequence comprised one cycle; this cycle was repeated for each sample to assess the shape-memory effect. Finally, the shape fixity (R_f) and the shape recovery (R_r) were calculated with the following equation:

$$R_f = (\varepsilon_u / \varepsilon_m) \times 100\%,$$

$$R_r = (\varepsilon_u - \varepsilon_p) / \varepsilon_u \times 100\%,$$

Where ε_u is the original unloading strain, ε_m is the original maximum strain, ε_p is the residual strain.

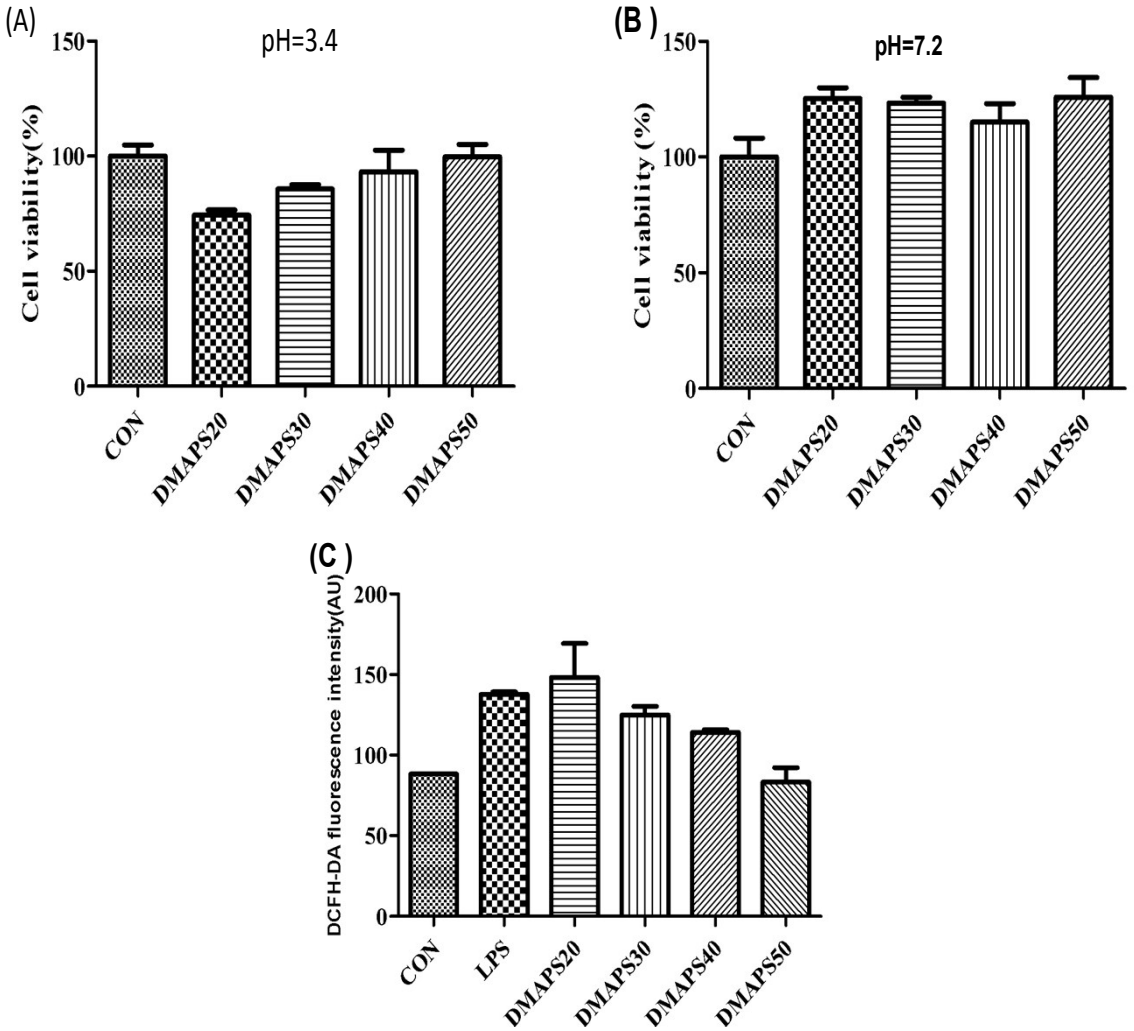

Figure SI7. Cell viability (5×10^5 cells/well in 24-well plates) incubated with 1mg/mL of p(DMAPS-co-AA) with different DMAPS-contents; A) pH=3.4; B) pH=7.2). C) ROS-production under same conditions as B). Control (CON)-untreated RAW264.7-cells; LPS (1µg/mL) was used as a positive control

The cytotoxic effects of poly(DMAPS-co-AA) are firstly assessed by measuring cell viability using a tertrazolium salt (WST-8)-based colorimetric assay in the Cell Counting Kit-8 (CCK-8). In this study, murine macrophage RAW264.7-cells are incubated with poly(DMAPS-co-AA) for analysis, since macrophages are involved in tissue remodeling during embryogenesis, wound repair, clearance of apoptotic cells, and hematopoiesis. Cell viability of the polymer solution treated cells was calculated by normalizing for untreated RAW264.7-cells. For the bulk poly(DMAPS-co-AA) solution with pH of 3.4, the cell viability of poly(DMAPS-co-AA) treated RAW264.7-cells is lower than that of control, while >85% cell viability is measured for DMAPS-content >30wt.%. Moreover, cell viability increases with increasing DMAPS-content, implying a low cytotoxicity in general.

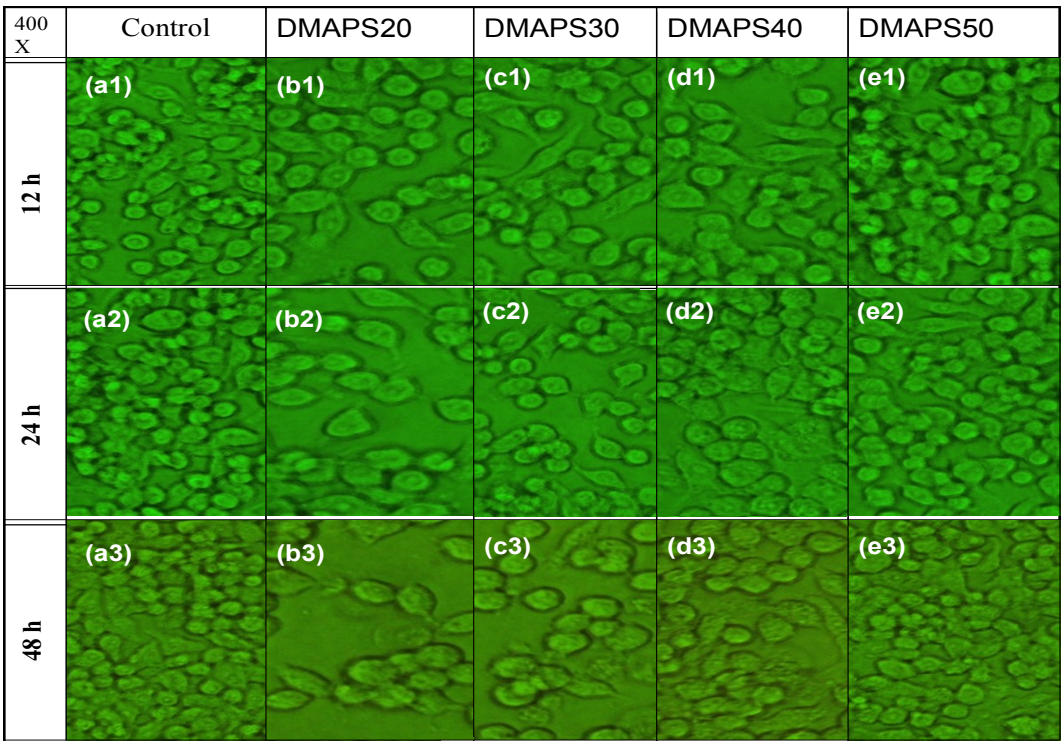

Figure SI8. inverted microscope images of RAW264.7 cells after incubating with Poly(DMAPS-co-AA) with different DMAPS-content for more than 48h

Inverted microscope images clearly show good cell growth after incubation with higher DMAPS-content samples after >48h**.**

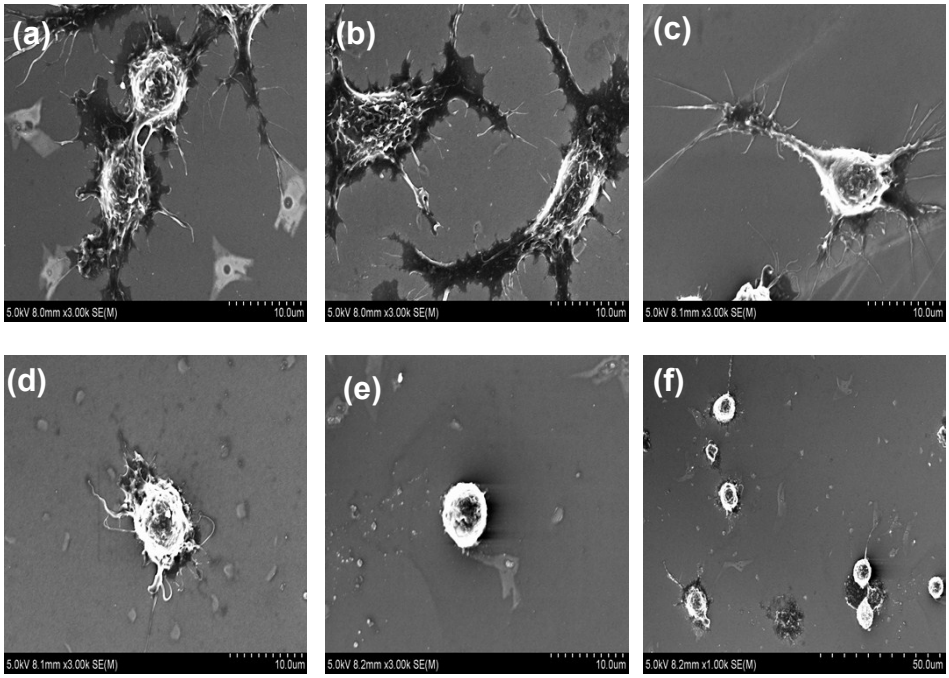

Figure SI9. SEM images showing the cell bioactivity of RAW264.7 cells incubated with poly(DMAPS-co-AA) with different DMAPS-contents at pH=3.4 (a-control, b-DMAPS50; c-DMAPS40; d-DMAPS30; e-DMAPS20; f-DMAPS20)

SEM-images also demonstrate that RAW264.7-cells incubated with DMAPS30, DMAPS40, and DMAPS50 adhere well on the substrate, having many clear pseudopodia, while cell contraction was found in the RAW264.7-cells incubated with DMAPS20, implying a bioactivity loss, possibly due to higher –COOH content or lower pH owing to higher AA-content. After adjusting the poly(DMAPS-co-AA)-solution to pH 7.2 by 1.0 mol L^{-1} NaOH, which significantly increases cell viability to 115%-130%, implying good biocompability for all poly(DMAPS-co-AA).

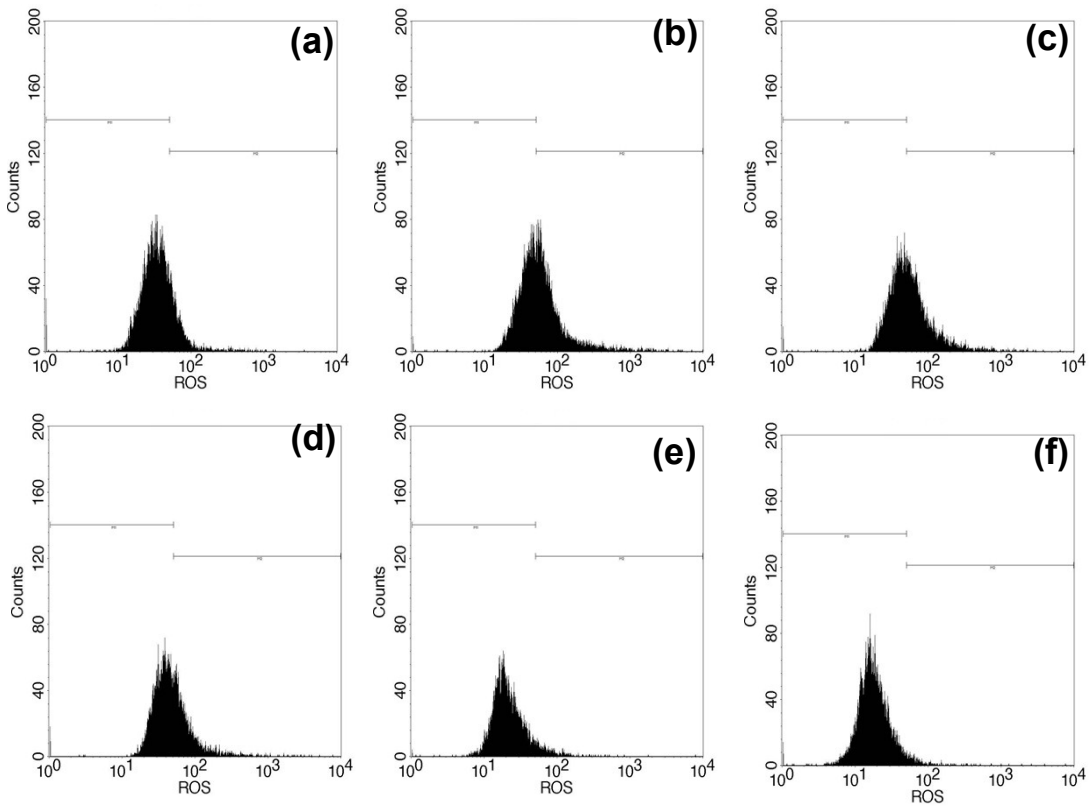

Figure SI10. Typical ROS value of RAW264.7 cells incubated with poly(DMAPS-co-AA) with different DMAPS-contents (a-control, b-LPS, c- DMAPS20; d-DMAPS30; e-DMAPS40; f-DMAPS50)

Additionally, intracellular accumulation of reactive oxygen species (ROS) was measured by fluorescent probe DSF-DA, typical for various diseases like atherosclerosis, diabetes, cancer, neurodegeneration as well as ageing. DCFH-DA fluorescence intensities for control and lipopolysaccharide (LPS) are ≈88 (AU) and ≈137 (AU), respectively. Except for DMPAS20, DCFH-DA fluorescence intensities is within 88-137AU**.** Moreover, as DMAPS-content increases, the DCFH-DA fluorescence intensity decreases significantly from 148AU for DMAPS20 to 109AU for DMAPS50, proving good biocompability for DMAPS-contents ≥30wt.%.

References

1. W.H. Kuo, M. J. Wang, H.W. Chien, T.C. Wei, C. Lee and W.B. Tsai, *Biomacromolecules*, 2011, **12**, 4348-4356.
2. D. Ratna and J. Karger-Kocsis, *Journal of Materials Science*, 2008, **43**, 254-269.
3. S. Chen, H. Yuan, Z. Ge, S. Chen, H. Zhuo and J. Liu, *Journal of Materials Chemistry C*, 2014, **2**, 1041-1049.